THE JOURNAL OF BIOLOGICAL CHEMISTRY VOL. 289, NO. 46, pp. 31867–31877, November 14, 2014

Drosophila Neuroligin3 Regulates Neuromuscular Junction Development and Synaptic Differentiation*◆

Received for publication, April 17, 2014, and in revised form, August 24, 2014 Published, JBC Papers in Press, September 16, 2014, DOI 10.1074/jbc.M114.574897

Guanglin Xing[1], **Guangming Gan**[1], **Dandan Chen, Mingkuan Sun, Jukang Yi, Huihui Lv, Junhai Han, and Wei Xie**[2]

From the Key Laboratory of Developmental Genes and Human Disease, Institute of Life Sciences, Southeast University, Nanjing 210096, China

Background: Postsynaptic neuroligins play essential roles in synaptic maturation and function.
Results: *Drosophila* Neuroligin3 regulates neuromuscular junction growth, GluRIIA recruitment, synaptic vesicle recycling, and postsynaptic density maturation.
Conclusion: This elucidates the *in vivo* roles of *Drosophila* Neuroligin3 in development and synaptic differentiation of NMJs.
Significance: This highlights that *Drosophila* can be used to understand and uncover functional diversity in neuroligins.

Neuroligins (Nlgs) are a family of cell adhesion molecules thought to be important for synapse maturation and function. Mammalian studies have shown that different Nlgs have different roles in synaptic maturation and function. In *Drosophila melanogaster*, the roles of *Drosophila neuroligin1* (DNlg1), *neuroligin2*, and *neuroligin4* have been examined. However, the roles of *neuroligin3* (*dnlg3*) in synaptic development and function have not been determined. In this study, we used the *Drosophila* neuromuscular junctions (NMJs) as a model system to investigate the *in vivo* role of *dnlg3*. We showed that DNlg3 was expressed in both the CNS and NMJs where it was largely restricted to the postsynaptic site. We generated *dnlg3* mutants and showed that these mutants exhibited an increased bouton number and reduced bouton size compared with the wild-type (WT) controls. Consistent with alterations in bouton properties, pre- and postsynaptic differentiations were affected in *dnlg3* mutants. This included abnormal synaptic vesicle endocytosis, increased postsynaptic density length, and reduced GluRIIA recruitment. In addition to impaired synaptic development and differentiation, we found that synaptic transmission was reduced in *dnlg3* mutants. Altogether, our data showed that DNlg3 was required for NMJ development, synaptic differentiation, and function.

Chemical synapses are the fundamental units of neuronal circuits and are important for virtually every aspect of nervous system function. Among the many molecules that are known to affect synapse formation and function, the trans-synaptic complex neurexin-neuroligin has captured special attention because of their trans-synaptic interaction property and has demonstrated synaptogenic effects (1–3). Human genetic studies have also indicated that neuroligins (Nlgs)[3] are linked to a number of neurodevelopmental and mental disorders such as autism and schizophrenia (4–6), underscoring the importance of these proteins in brain development and function.

Nlgs were initially identified as the postsynaptic partners for the presynaptic protein neurexin (7–9). In mice, there are four neuroligin genes (*Nlg1–4*), although Nlg1 and Nlg2 are preferentially expressed at excitatory and inhibitory synapses, respectively (10, 11), and Nlg3 is present at both types of synapses (12). When expressed in cultured non-neuronal cells, Nlgs can trigger the assembly of presynaptic specialization (2). In addition, overexpression of Nlgs in cultured neurons increases the number of synapses and potentiates synaptic function (1, 13–15). These *in vitro* results suggest that Nlgs may play a key role in synapse formation. However, recent *in vivo* studies in mice showed that although deletion of Nlgs drastically affects synaptic strength, it has minimal effect on synapse number (16). These results have led to the proposal that Nlgs are specifically important for synaptic maturation and function but not for initial synapse formation (13, 17). Interestingly, a more recent study using a combination of sparse knockdown of *Nlg1* and two-photon glutamate uncaging showed that Nlg1 does play an essential role in activity-dependent spinogenesis and does regulate cortical synaptogenesis and synapse number (18).

Compared with the mammalian brain, *Drosophila* NMJs provide a relatively simpler and genetically more amenable system to dissect the molecular mechanisms underlying synapse development and maturation. Similar to mammals, the *Drosophila* also has four Nlgs (*dnlg1–4*) (19, 20). We and others have previously shown that although DNlg1 is specifically expressed at NMJs, DNlg2 is expressed in both NMJs and CNS, and loss of either *dnlg1* or *dnlg2* causes deficits in bouton development (*i.e.* reduced bouton number) and postsynaptic assembly (19–21). Our more recent study about *dnlg4* suggests that DNlg4 is expressed in large ventral clock neurons and is essen-

* This work was supported by Natural Science Foundation of China Grant 31171041, National Basic Research Program (973 Program) Grant 2012CB517903, and Natural Science Foundation of China and Canadian Institutes of Health Research Joint Health Research Initiative Program Grant 81161120543 (to W. X.).
◆ This article was selected as a Paper of the Week.
[1] Both authors contributed equally to this work.
[2] To whom correspondence should be addressed: Institute of Life Sciences, Southeast University, 2 Sipailou Rd., Nanjing 210096, China. Tel.: 86-25-83790970; Fax: 86-25-83790970; E-mail: wei.xie@seu.edu.cn.

[3] The abbreviations used are: Nlg, neuroligin; DNlg, *Drosophila* neuroligin; NMJ, neuromuscular junction; GluRIIA/IIB, glutamate receptor IIA/IIB; EJP, evoked junction potential; mEJP, miniature excitatory junction potential; PSD, postsynaptic density; SSR, subsynaptic reticulum; Brp, Bruchpilot; FasII, fasciclin II; DLG, Dics large 1; VNC, ventral nerve cord; Syt, synaptotagmin.

tial for sleep regulation (22). These results support a critical role for DNlgs in synaptic development and maturation. However, the roles of *dnlg3* have yet to be determined.

In this study, we investigated the role of DNlg3 at *Drosophila* NMJs by generating and analyzing *dnlg3* mutant flies. To our surprise, we found that *dnlg3* null mutants had an opposite effect on bouton development compared with *dnlg1* or *dnlg2* null mutants. In addition, pre- and postsynaptic differentiations were impaired in *dnlg3* mutants, such as abnormal synaptic vesicle endocytosis, increased PSD length, and reduced GluRIIA level. These results suggest that DNlg3 plays important roles in NMJ development and synaptic differentiation.

EXPERIMENTAL PROCEDURES

Fly Stocks and Cloning of Full-length dnlg3 cDNA Clones—The muscle-specific line 24B-Gal4 was obtained from the Kyoto stock center. PBac{WH}CG34127^{f00777} (abbreviated as *dnlg3*^{f00777}), MHC-Gal4, and Elav-Gal4 were obtained from Bloomington stock center. *UAS-DNlg3* transgenic flies were generated by injecting w^{1118} with a pUAST vector containing the full-length DNlg3 protein coding sequence. *Elav-Gal4/+(Y);dnlg3*^{KO88}*/dnlg3*^{KO127}*,UAS-DNlg3* and *MHC-Gal4/+(Y); dnlg3*^{KO88}*/dnlg3*^{KO127}*,UAS-DNlg3* flies were used as neuron- and muscle-specific rescue lines. In this study, w^{1118} flies were used as wild-type (WT) controls.

Generation of dnlg3 Null Mutant—The Ends-out technology used to knock out the *dnlg3* gene was described previously (20, 23). Briefly, two pairs of primers (5′-ATCCGTACGGGCAATGAAGAGAAGCAGAT-3′ and 5′-ATCGGCGCGCCCTGCTGCGTTTTCTGAATGC-3′; 5′-ATCGGTACCCTGTCACCTGTCTGCCCTTT-3′ and 5′ATCGCGGCCGCGTTGCTGCTCCATTCCCACG-3′) were used to amplify two homologous fragments (upstream arm, −4739 to −1556; downstream arm, 2293–5243) of the *dnlg3* locus from w^{1118} genomic DNA. These fragments were then subcloned into the PW25 vector, and the recombinant vector was used for injecting the w^{1118} embryos. Virgin donor flies bearing the targeting construct on the third chromosome were crossed to yw; P(70hsFLP70hsI-SceI)/Cyo (Bloomington stock center 6934) flies and the first-instar progeny larvae were heat-shocked for 90 min at 38 °C to induce homologous recombination. DNA primers (5′-CGCTGCTTTGTCGTGGGTAA-3′ and 5′-TGGTTCCGAGTGGTTCATTT-3′) were used for screening and confirming the targeted flies. Two independent targeted mutant lines, *dnlg3*^{KO88} and *dnlg3*^{KO127}, were obtained.

Adult and Larval Locomotion—For adult locomotor activity assay, 2–4-day-old male flies raised in standard food were placed in 51 × 5-mm transparent tubes with enough food. Locomotor activity was monitored by MB5 MultiBeam Activity Monitor (Trikinetics), and 17 independent IR beams per tube were used to detect activity. Locomotor activity was tracked as numbers of beam-crossings per unit of time, usually 1-min intervals. We chose time 19:00–20:00 for statistic assay, because of high locomotor activity in this time range.

To monitor larval locomotion, transparent dishes (diameter, 15 cm) with 6% agar substrate were used as an arena for crawling larvae. Grape juice was added until the substrate obtained a dark purple color. In each trial, a single wandering third-instar larva was chosen from the vial and transported to the center of the arena. The movement of larvae was visualized via a standard commercial video camera (resolution >640 × 480) for 3 min. Tracker software was written in Python to track the trajectory, and 3-min trajectory distances were calculated for assessing larval locomotion activity.

Antibody Production, Western Blot Analysis—To generate a DNlg3 monoclonal antibody, a recombinant protein containing C-terminal 119 amino acids (His-1011 to Gln-1129) fused with the His_6 tag at the N terminus was used as an antigen. The same C-terminal amino acids fused with glutathione *S*-transferase were used for screening for the monoclonal cells bearing the antibody. The specificity of the antibody was confirmed by using *dnlg3* null mutant flies.

The procedure for Western blot analysis was described previously (20). In brief, adult fruit fly heads, ventral nerve cord (VNC), and muscle filament were homogenized with 1× SDS loading buffer (50 mM Tris-HCl, 2% SDS, 0.1% bromphenol blue, 10% glycerol, 1% β-mercaptoethanol), and the total protein lysates were separated on an 8% SDS-polyacrylamide gel and electrotransferred onto polyvinylidene difluoride membranes. Immobilized proteins on the membrane were probed with primary antibodies at 4 °C overnight. The primary antibodies used for Western blot analysis were anti-DNlg3 (1:1000), anti-DNrx (1:400), anti-GluRIIA (DSHB; 1:30), anti-DLG (DSHB; 1:1000), and anti-tubulin (DM1A; Sigma 1:8000). The samples were then incubated with HRP-conjugated secondary antibodies at room temperature for 1 h, and the targeted proteins were visualized with the Qentix Western signal enhancer and SS West Pico substrate detection system (Thermo Scientific).

Immunochemistry—Immunostaining of larval or embryonic samples was performed as described previously (20). Briefly, fixed samples were washed four times in 0.3% PBST (PBS + 0.3% Triton X-100) rapidly, blocked in the blocking solution for 1 h, incubated with primary antibody at 4 °C overnight, followed by appropriate secondary antibodies for 1 h at room temperature. The following primary and secondary antibodies were used: rabbit anti-HRP (1:1000; Jackson ImmunoResearch, West Grove, PA); rabbit anti-GluRIII (1:2500) and rabbit anti-GluRIIB (1:2000; gifts from A. DiAntonio, Washington University, St. Louis, MO); mouse anti-Brp (nc82; 1:25; DSHB), mouse anti-GluRIIA (8B4D2; 1:25; DSHB), mouse anti-DLG (4F3; 1:50; DSHB), mouse anti-FasII (1D4;1:25; DSHB), and mouse anti-synaptotagmin (3H2D7; 1:25; DSHB); and fluorophore-conjugated secondary antibodies (Invitrogen, 1:500). Following the antibody incubation, the samples were washed extensively and mounted in VectaShield mounting medium (Vector Laboratories). All images were collected using a Carl Zeiss LSM 510 confocal station and analyzed with ImageJ software (National Institutes of Health).

For the analysis of NMJs, wandering third-instar larvae were selected and dissected. For quantifications of the bouton number, dissected body wall muscle samples were stained with HRP and DLG, and the NMJs of muscle 4 of abdominal segments 3 and 4 were collected. For quantifications of bouton size, the three biggest boutons of type Ib boutons at NMJ4 were measured using ImageJ software (National Institutes of Health).

Electrophysiological Recordings—Procedures for conventional intracellular recordings for assessing NMJ neurotransmissions were described previously (20). Briefly, wandering third instar larvae were dissected in Ca^{2+}-free HL3.1 saline and recorded in HL3.1 saline containing 0.8 mM Ca^{2+}. Microelectrodes (20–50 megohms) were pulled from the borosilicate glass (WPI) with a glass puller (P-2000; Sutter Instruments) and filled with 3 M KCl. Recording were performed at 20–22 °C with an axoclamp 2B amplifier (Molecular Devices) in Bridge mode. Recording data were collected with pClamp9.1 software (Molecular Devices) and digitized by a digitizer 1322A (Molecular Devices). EJPs were evoked with a Grass S48 stimulator (Astro-Grass Inc) at 0.3 Hz with supra-threshold stimulating pulses and were obtained at muscle 6 of abdominal segment 3. Five EJP responses were collected for each animal. Miniature EJPs (mEJPs) were recorded for a period of 120 s after the EJP recording. Data were processed with mini-analysis (Synaptosoft) software and statistically evaluated with SigmaPlot software. Only the recordings with resting membrane potentials ranging from −60 to −65 mV were used for analysis.

EM—The methods for third-instar larval NMJ6/7 EM used in this study were described in previous reports (20, 24). In brief, third-instar larvae were rapidly dissected in Ca^{2+}-free HL3.1 solution (in mM: 70 NaCl, 5 KCl, 4 $MgCl_2$, 10 $NaHCO_3$, 5 trehalose, 115 sucrose, and 5 HEPES, pH 7.2). The dissected third-instar body wall muscles (NMJ 6/7; segment A3) were first fixed for 4 h at 4 °C in 2% glutaraldehyde and 2% paraformaldehyde in 0.1 M sodium cacodylate buffer, pH 7.2. The samples were then fixed at 4% glutaraldehyde overnight. After overnight fixation, the samples were washed four times with washing buffer (0.1 M sodium cacodylate buffer, pH 7.2), and postfixed for 1.5 h with washing buffer containing 1% osmium tetroxide. After washing rapidly three times in distilled water, the samples were stained for 1 h on ice with 1% uranyl acetate in distilled water. After washing rapidly one time with distilled water, samples were dehydrated at room temperature with increasing ethanol concentrations, infiltrated in Epon resin (first in 100% EtOH/Epon at 1:1, for 30 and 90 min, and then in 100% Epon overnight), and embedded in three successive steps at 30, 45, and 60 °C, each lasting for 24 h. The samples were then trimmed. Series of 80-90-nm ultrathin sections were cut with a 35° diamond knife (Diatome) on a Reichert ultracut ultramicrotome (Leica) and mounted on Formvar-coated grids. The sections were finally stained in uranyl acetate and lead citrate. Micrographs were obtained with a Philips EM 301 transmission electron microscope.

FM1-43 Uptake Assay—Procedures for FM1-43 loading and unloading assays were described previously (25). Wandering third-instar larvae were dissected in Ca^{2+}-free HL-3 solution and washed with the same solution. To load the fluorescent FM1-43 dye, the samples were stimulated by adding a high K^+ (90 mM) solution containing 4 μM FM1-43 dye and 1.5 mM Ca^{2+} for 2 min. The samples were then washed five times with Ca^{2+}-free HL-3 solution for 5 min. The loaded NMJ were collected by a Carl Zeiss LSM 510 confocal station with a ×40 water-immersion lens. For unloading assay, the same NMJs were used and were rested for 5 min, and high K^+ solution without FM1-43 dye was added to the samples for 1 min to elicit exocytosis and then washed five times for 5 min with a generous amount of HL-3 solution without Ca^{2+}. The components of HL-3 solution were as follows: 110 mM NaCl, 5 mM KCl, 10 mM $NaHCO_3$, 5 mM HEPES, 30 mM sucrose, 5 mM trehalose, 10 mM $MgCl_2$, pH 7.2. High K^+ solution contained 90 mM KCl, whereas NaCl was reduced by an equivalent amount.

Quantification of Fluorescence Intensity—For comparisons of fluorescent intensities between genotypes, all samples were dissected and fixed under identical conditions, processed in the same vials, and collected under the same microscope setting, and all assays were repeated at least three times. For each channel, the sum of pixel intensities was recorded by software ImageJ. We used anti-HRP staining as control (20, 26). The ratio of anti-Brp/anti-HRP, anti-DLG/anti-HRP, anti-synaptotagmin/anti-HRP, anti-fasciclin II/anti-HRP, anti-GluRIIA/anti-HRP staining intensity was calculated for each genotype in Fig. 5. Two NMJs at NMJ6/7 of A2 segment of each animal were analyzed.

RESULTS

Reduced Locomotor Activity in dnlg3 Null Mutants—The *Flybase* information on the *dnlg3* gene (CG34127) indicates that the gene is located on the right arm of chromosome three at a cytological position at 84D10–84D11 spanning approximately a 60-kb DNA fragment with 14 exons and 13 introns, and it encodes a protein of 1159 amino acids. The DNlg3 protein is predicted to have all of the typical domains found within Nlgs, including an N-terminal signal peptide, an acetylcholinesterase-like domain, a single transmembrane domain, and a C-terminal domain containing a PDZ-binding motif (Fig. 1*A*). To address the *in vivo* function of the *dnlg3*, we used the Ends-out method to generate *dnlg3* knock-out mutants whereby 3849 bp of a *dnlg3* genomic DNA fragment (−1556–2293 bp) was replaced by a mini-white gene (Fig. 1, *B* and *C*). Because the donor construct was docking on chromosome 3, the same chromosome as the *dnlg3* gene, we used PCR analysis to screen knock-out mutants, and the PCR primers F1 and R1 are shown in Fig. 1*C*. As predicted, an ~5.7-kb band was obtained in mutants but not in the control flies (Fig. 1*D*). Two independent knock-out lines, $dnlg3^{KO88}$ and $dnlg3^{KO127}$, were obtained. Western blots and immunostaining assays were used to analyze DNlg3 expression in *dnlg3* mutants. It is important to note that our antibody detected two major bands in WT flies (a predicted 130 kDa and a smaller 90 kDa), suggesting that the protein might undergo extensive post-translational modifications, but importantly, both forms were absent in the null mutants flies (Fig. 1*E*). It was also noted that the *piggybac* of PBac{WH}$CG34127^{f00777}$ insertion also disrupted DNlg3 expression (Fig. 1*E*). Immunostaining results showed that in the embryonic and larval stage, DNlg3 protein was enriched in the central nervous system but absent in *dnlg3* mutants (Fig. 1, *F*–*I*′).

The *dnlg3* mutants were viable and fertile with no obvious abnormalities in body size or morphology; however, both larvae and adults of *dnlg3* mutants showed reduced locomotor activity (Fig. 1, *J* and *K*), which might suggest impaired synaptic function at the neuromuscular junction or in the central nervous system.

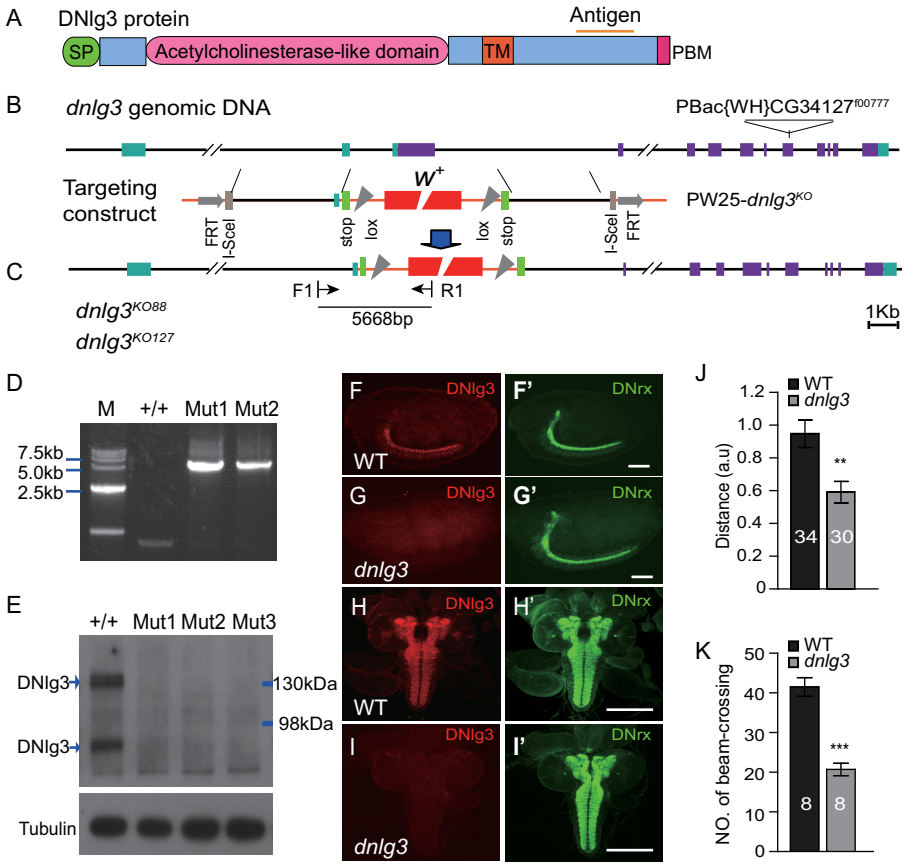

FIGURE 1. **Reduced locomotor activity in *dnlg3* mutants.** *A,* schematic diagram of DNlg3 protein structure and antigenic site. DNlg3 protein contains the following domains: signal peptide (*SP*), acetylcholinesterase-like domain, transmembrane domain (*TM*), and PDZ domain-binding motif (*PBM*). *B* and *C,* schematic diagram of Ends-out targeting of *dnlg3*. *B,* genomic structure of the *dnlg3* gene showing exons, PBac{WH}CG34127^{f00777}position, and targeting vector. *C,* targeted locus and position of primers used for screening for the targeted mutant flies. *D,* PCR analysis of WT(+/+), *dnlg3*^{KO88} (*Mut1*), and *dnlg3*^{KO127} (*Mut2*) genomic DNA using primers shown in *C* showing the presence of a predicted band of 5.7 kb in the targeted mutants but not in WT. *M*, marker. *E,* Western blot analysis of protein lysates prepared from fly heads using our anti-DNlg3 antibody showing the presence of two major bands (130 and 90 kDa) in WT but not in the targeted mutants and in *dnl3*^{KO127f00777} (*Mut3*) mutants. *F–I′*, immunostaining confirming the absence of *dnlg3* gene expression in *dnlg3* null mutants. Note high levels of expression of DNlg3 in WT embryonic central nervous system (*F*) and in third-instar larvae central nervous system (*H*) but absent in the *dnlg3* mutant (*G* and *I*). *J,* summary *graph* showing a 3-min crawling distance in the third-instar larvae of WT and *dnlg3* mutants. Note that *dnlg3* mutants showed reduced crawling distance, compared with WT controls (*a.u.*, artificial unit). *K,* adult locomotor assay showing a reduced 1-min number of beam-crossing in *dnlg3* mutants, compared with WT controls. **, $p < 0.01$; ***, $p < 0.001$, Mann-Whitney test. *Scales bars: B* and *C,* 1 kb; *F–G′*, 100 μm; *H–I′*, 200 μm.

Normal Expression and Localization of DNrx in dnlg3 Mutants—Because of a low level of DNlg3 protein at the NMJs or a low affinity of the DNlg3 antibody, we were not able to detect any endogenous DNlg3 immunoreactivity signals at WT NMJs. We therefore generated a DNlg3 overexpression line with a muscle-specific MHC-Gal4 in a WT background. In this line, DNlg3 protein was seen to be concentrated at type I boutons, and co-localized with DLG signals (Fig. 2, *A* and *A″*). To confirm whether DNlg3 is expressed at the body wall muscle endogenously, we carefully dissected wild-type larval VNC and body wall muscle tissues, respectively, and extracted mRNA from both tissues, and then we performed reversed PCR using *dnlg3* primers and β-tubulin primers. It is shown that both VNC and body wall muscle have *dnlg3* mRNA (Fig. 2*B*). These results suggest that DNlg3 was expressed at body wall muscle and can be targeted to postsynapse at NMJs.

As we know *Drosophila* has only one neurexin gene, *dnrx* (27, 28), we wanted to know whether DNrx expression and localization are altered in *dnlg3* mutants. First, we examined expression and localization of DNrx in both WT and *dnlg3* mutants central nerve system. Similar to WT, DNrx could be targeted to the synapse-rich region and neuropil region in *dnlg3* mutants (Fig. 1, *F–I′*), and the level of DNrx protein was not changed (Fig. 2*E*).

To examine DNrx localization at NMJs, the full-length cDNA of DNrx transgenic flies was used and expressed in presynaptic motoneurons. Overexpressing DNrx with OK6-Gal4 in both wild-type and *dnlg3* mutants showed that the localization of DNrx in both lines was similar (Fig. 2, *C–D″*). These results indicated that DNrx expression and localization were not altered in *dnlg3* mutants.

Impaired Synaptic Transmission in dnlg3 Null Mutants—As postsynaptic adhesion molecules, Nlgs play essential roles in synaptic transmission (13, 16). To investigate whether synaptic transmission was affected in *dnlg3* mutants, we performed electrophysiological recordings at NMJs of the third instar larvae. We examined both evoked and spontaneous responses under approximately physiological conditions containing 0.8 mM Ca^{2+}. We found that the amplitudes of both excitatory junction potential (EJPs) and miniature excitatory junction potential (mEJP) frequencies were significantly reduced in *dnlg3*^{KO127} mutants compared with the WT controls (Fig. 3, *A–E*). Similar

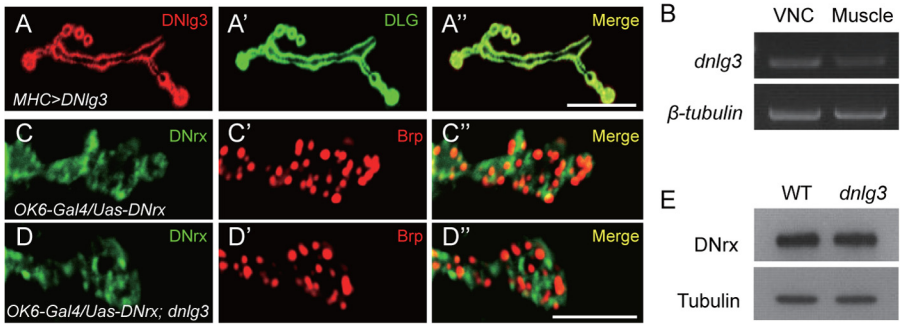

FIGURE 2. **Postsynaptic localization of DNlg3 at NMJs and normal expression and localization of DNrx in *dnlg3* mutants.** *A–A″*, type Ib boutons costained with anti-DLG and anti-DNlg3 antibodies showing overlapping expression of DNlg3 and DLG in the *MHC>DNlg3* line. *B*, reverse PCR analysis of *dnlg3* and *β*-tubulin gene expression in wild-type VNC and body wall muscle tissues (*Muscle*) showing *dnlg3* expression at both VNC and body wall muscles. Primers used for the *dnlg3* gene were 5′-GAGTATACGGATTGGGAGAGG-3′ and 5′-TTCGGTTTTCGTGTAGTTGC-3′; primers used for the *β*-tubulin gene were 5′-ATGGACTCT-GTGCGATCGGG-3′ and 5′-TTAGTTCTCGTCGACCTCAG-3′. *C–D″*, overexpression of DNrx with motoneuron OK6-Gal4 in both wild-type and *dnlg3* mutant showing DNrx localization in both lines was similar. *E*, Western blot analysis of protein lysates prepared from WT and *dnlg3* mutants larval VNC using anti-DNrx and anti-tubulin showing normal DNrx expression in *dnlg3* mutants. *Scales bars: A–A″*, 20 μm; *C–D″*, 5 μm.

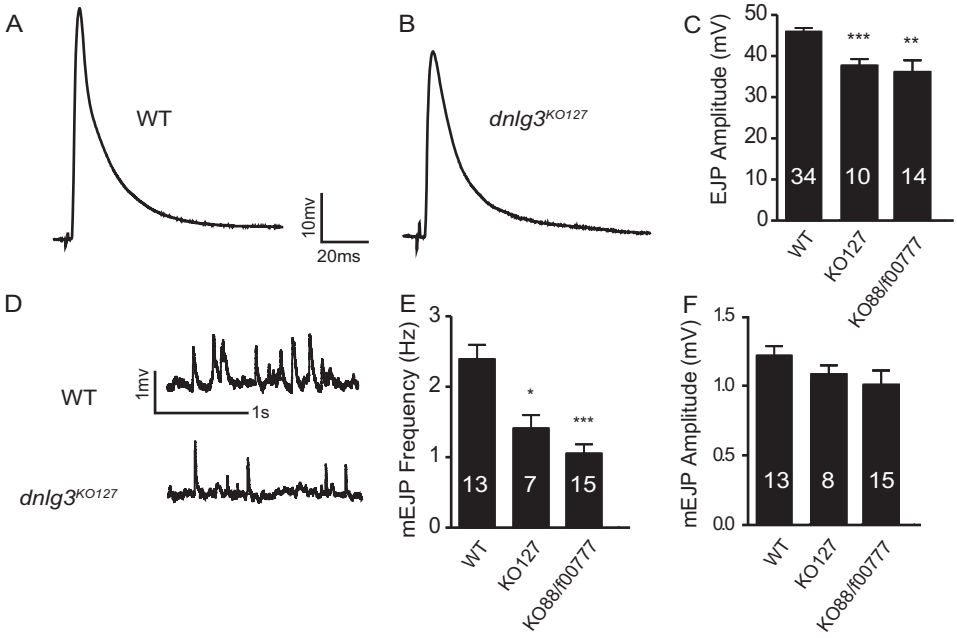

FIGURE 3. **Impaired synaptic transmission in *dnlg3* mutants.** *A–B*, representative traces of EJPs recorded from muscle 6 in abdominal segment 3 in the presence of 0.8 mM calcium in WT, *dnlg3*^{KO127}. *C*, summary *graph* showing significantly reduced EJP amplitude in *dnlg3* mutants (*dnlg3*^{KO127} and *dnlg3*$^{KO88/f00777}$), compared with WT controls. *D*, representative traces of mEJPs recorded from muscle 6 in abdominal segment 3 in the presence of 0.8 mM calcium in WT, *dnlg3*^{KO127}. *E*, summary *graph* showing reduced mEJPs frequency in *dnlg3* mutants, compared with WT controls. *F*, summary *graph* of mEJP amplitudes showing no significant differences between WT and *dnlg3* mutants. The number of samples analyzed is indicated. *, $p < 0.05$; **, $p < 0.01$; ***, $p < 0.001$, Mann-Whitney test.

results were seen in *dnlg3*$^{KO88/f00777}$ mutants (Fig. 3, *C* and *E*), indicating that those phenotypes are caused by *dnlg3* mutation. We also found that the mEJP amplitudes were decreased slightly but not significantly altered in *dnlg3* mutants compared with WT controls (Fig. 3*F*). Thus, the properties of synaptic transmission were altered in *dnlg3* mutants.

Increased Bouton Number and Decreased Bouton Size in dnlg3 Null Mutants—In vivo studies in mice have shown that loss of Nlgs results in impaired synaptic transmission and plasticity but with no significant changes in synapse formation or synaptic morphology (13, 16, 29). In *Drosophila,* however, both DNlg1 and DNlg2 have been shown to be important for both NMJ development and function; loss of *dngl1* or *dnlg2* resulted in reduced bouton number, altered synaptic structures, and impaired synaptic transmission (19–21). To determine whether the reduced synaptic transmission observed in *dnlg3* mutants was caused by morphological changes in synaptic number or synaptic development, we first analyzed the overall morphology of NMJs in both *dnlg3* null mutants and WT controls by co-labeling the NMJ with anti-HRP and anti-DLG antibodies, noting that HRP and DLG are a pan-neuronal and a postsynaptic subsynaptic reticulum (SSR) marker used for assessing presynaptic bouton and postsynaptic properties, respectively. To facilitate quantitative analysis, we focused on type Ib boutons in muscle 4 of abdominal segment 3/4. Previous studies have shown that NMJs in muscle 4 have more than two dozen type Ib boutons with large sizes and display a stereotypic branching pattern (27). Specifically, we analyzed bouton number and bouton size in the third-instar larvae. Similar to *dnlg1* and *dnlg2* mutants, synaptic boutons were formed in *dnlg3*

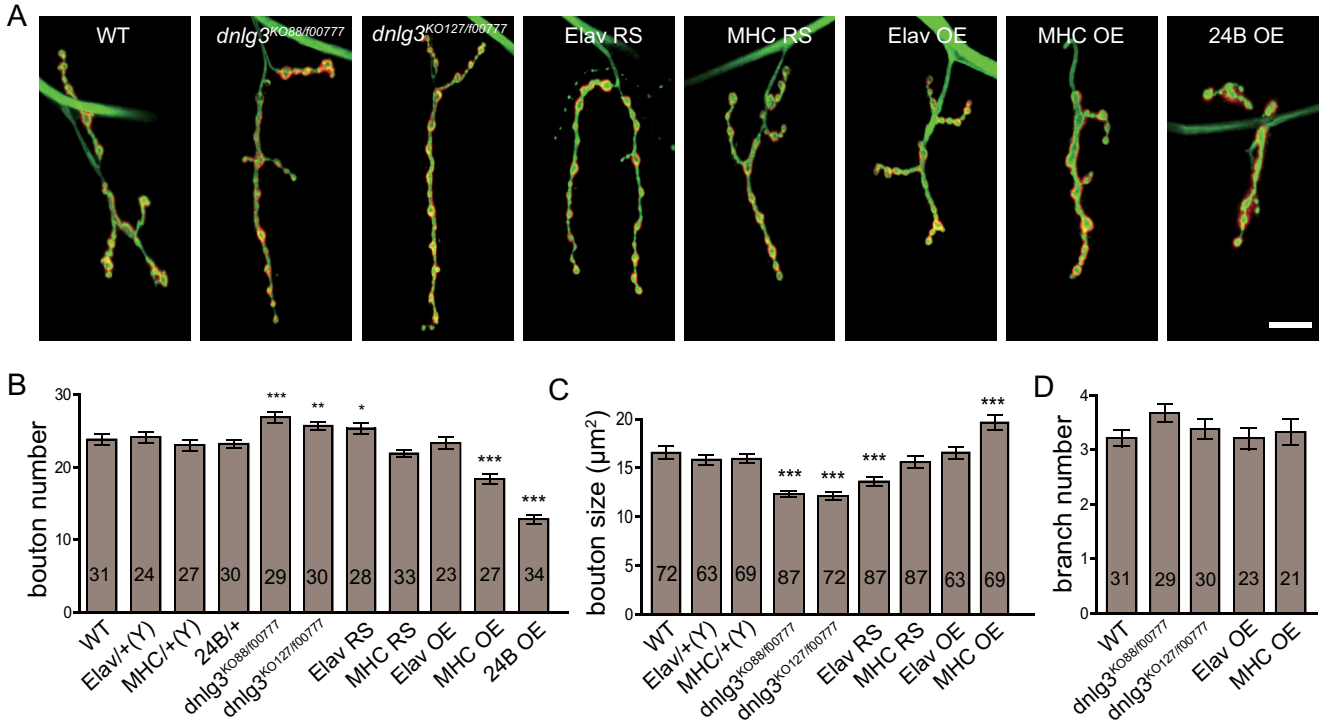

FIGURE 4. **Increased bouton number and reduced bouton size in *dnlg3* null mutants and reduced bouton number and increased bouton size in *dnlg3* overexpression lines.** *A,* confocal images of type Ib boutons at muscle 4 of abdominal segment 3 and segment 4 costained with anti-HRP and anti-DLG showing bouton phenotypes in WT, *dnlg3* null mutants ($dnlg3^{KO88/f00777}$ and $dnlg3^{KO127/f00777}$), a neuron-specific rescue line using Elav-Gal4 (*Elav RS*), a muscle-specific rescue line using MHC-Gal4 (*MHC RS*), a neuron-specific overexpression line (*Elav OE*), and two muscle-specific overexpression lines (*MHC OE* and 24B OE). *B,* summary *graph* showing a significant increase in bouton number in $dnlg3^{KO88/f00777}$ and $dnlg3^{KO127/f00777}$ compared with the WT control, complete rescue of the increased bouton number by the muscle-specific MHC-Gal4, and a significant decrease in bouton number in the muscle-specific overexpression lines MHC OE and 24B OE compared with the WT control. Note that the increased bouton number in *dnlg3* null mutants was not rescued by the neuron-specific Elav-Gal4 and that the neuron-specific overexpression line Elav OE did not cause significant changes in bouton number. *C,* summary *graph* showing significantly reduced bouton size in $dnlg3^{KO88/f00777}$ and $dnlg3^{KO127/f00777}$, rescue of the reduced bouton size by the muscle-specific MHC-Gal4, significantly increased bouton size in the muscle-specific overexpression line MHC OE. Note again that the reduced bouton size in *dnlg3* null mutants was only slightly affected by the neuron-specific Elav RS and that the neuron-specific overexpression line Elav OE did not cause significant changes in bouton size. *D,* summary *graph* of branch numbers showing no differences between genotypes. The number of samples analyzed is indicated. *, $p < 0.05$; **, $p < 0.01$; ***, $p < 0.001$, Mann-Whitney test. *Scales bar: A,* 20 μm.

mutants, and the overall pattern of innervations appeared normal. However, different from *dnlg1* and *dnlg2* mutants, *dnlg3* null mutants showed an increase in bouton number and a decrease in bouton size compared with WT controls (Fig. 4, *A*–*C*). These changes could be rescued with the muscle-specific MHC-Gal4 but not by neuron-specific Elav-Gal4 (Fig. 4, *A*–*C*). To determine whether the increased bouton numbers were attributable to the increased extent of synaptic arboration in *dnlg3* mutants, we measured the branch numbers and found that branch numbers were similar in all genotypes (Fig. 4*D*). These results suggested that DNlg3 plays a distinct role from DNlg1 and DNlg2 in NMJ development/maturation.

Decreased Bouton Number and Increased Bouton Size in DNlg3 Overexpression Lines—In vitro studies have indicated that overexpression of the mammalian Nlgs and their partners, Nrxs, induces new synapse formation and increased synapse number in culture cells (2, 3, 10, 30). In *Drosophila,* neuronal expression of DNrx in a WT background promotes proliferation of synaptic boutons (27), and overexpression of DNlg2 with actin-Gal4 also increases bouton growth (21). However, overexpression of DNlg1 with muscle-specific Mef2-Gal4 leads to a decrease of bouton growth due to interference with presynaptic DNrx function (19). To test whether DNlg3 could exert a positive effect in promoting growth of NMJs, we expressed DNlg3 with both neuron- and muscle-specific Gal4 drivers in a WT background. As shown in Fig. 4*A*, overexpression of DNlg3 with the Elav-Gal4 driver did not result in any significant changes in bouton number or bouton size compared with WT controls. However, overexpression of DNlg3 with muscle drivers significantly reduced bouton numbers (Fig. 4, *A* and *B*). In addition, the reduction in bouton numbers appeared to be correlated with the amount of DNlg3; expression of DNlg3 using one copy of MHC-Gal4 resulted in an ~30% reduction in bouton number, whereas DNlg3 expression using one copy of 24B-Gal4 resulted in about a 50% reduction in the bouton numbers, noting that MHC-Gal4 is a weak Gal4 but 24B-Gal4 is a strong Gal4 (31). Expression of DNlg3 using two copies of the 24B-Gal4 drivers with two copies of the UAS-DNlg3 resulted in larval lethality (data not shown). In contrast to *dnlg3* null mutants, overexpression of DNlg3 with MHC-Gal4 significantly increased bouton size compared with WT (Fig. 4, *A* and *C*). Because the bouton morphology in the 24B-Gal4 driver line was abnormal (Fig. 4*A*), we were not able to quantify the bouton size in this line. Also the branch numbers were not altered in overexpression lines (Fig. 4*D*). Both loss-of-function and gain-of-function studies suggested an important role of DNlg3 in the development/maturation of NMJs.

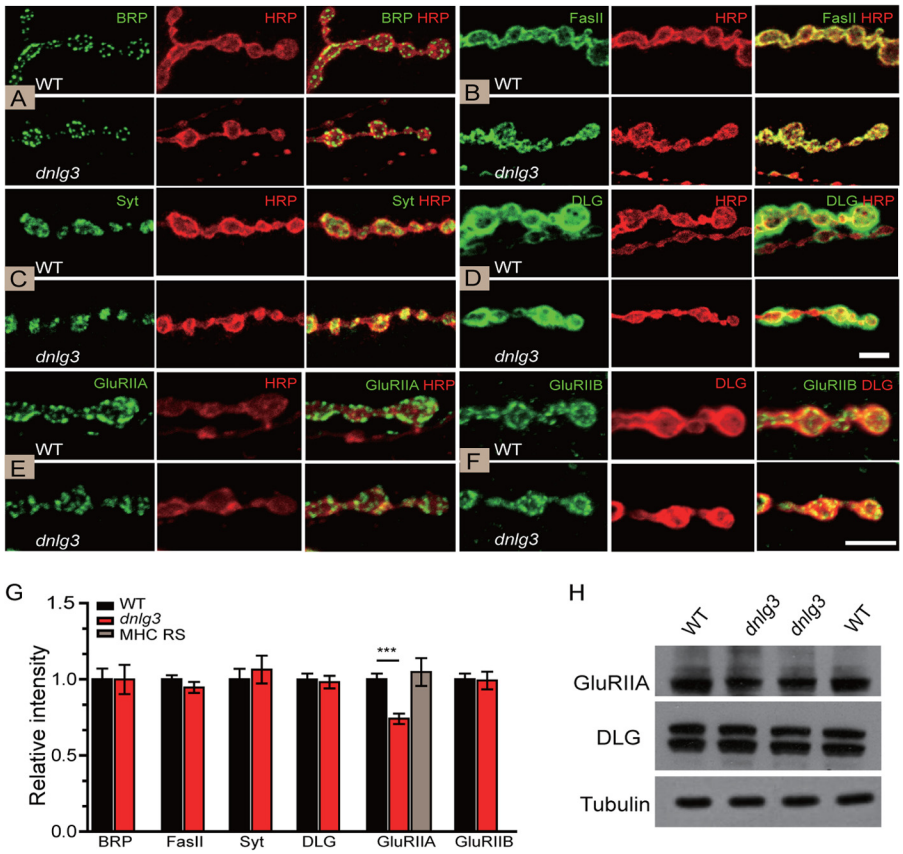

FIGURE 5. **Impaired GluRIIA recruitment and normal distribution and protein levels of Brp, FasII, Syt, DLG, and GluRIIB in *dnlg3* mutants.** *A–F,* type Ib boutons at NMJ6/7 of segment A3 costained for the active marker Brp and HRP in WT ($n = 9$) and *dnlg3* mutants ($n = 9$) (*A*); synaptic adhesion molecule fasciclin II (*FasII*) and HRP in WT ($n = 9$) and *dnlg3* mutants ($n = 9$) (*B*); synaptic vesicle protein Syt and HRP in WT ($n = 9$) and *dnlg3* mutants ($n = 9$) (*C*); subsynaptic reticulum marker DLG and HRP in WT ($n = 9$) and *dnlg3* mutants ($n = 9$) (*D*); GluRIIA and HRP in WT ($n = 8$) and *dnlg3* mutants ($n = 8$) (*E*); GluRIIB and DLG in WT ($n = 8$) and *dnlg3* mutants ($n = 8$) (*F*). Note that the distribution and protein levels of Brp, FasII, Syt, DLG, and GluRIIB were normal in *dnlg3* mutants compared with WT controls, and although the distribution of GluRIIA was normal, protein level was significantly reduced in *dnlg3* mutants compared with WT controls. *G,* summary *graph* showing relative protein levels. Note again that GluRIIA protein level was reduced in *dnlg3* mutants compared with WT controls, complete rescue of the reduced GluRIIA by the MHC RS. *H,* Western blot analysis of protein lysates prepared from larval body wall muscles using anti-GluRIIA, anti-DLG, and anti-tubulin antibodies showing reduced GluRIIA levels in *dnlg3* mutants. ***, $p < 0.001$, Mann-Whitney test. *Scales bars: A–D,* 5 μm; *E* and *F,* 5 μm.

Impaired Postsynaptic GluRIIA Targeting in dnlg3 Null Mutants—To clarify the function of DNlg3 in synaptic maturation, the expressions of some synaptic proteins were analyzed in *dnlg3* mutants. We examined active zone protein Brp (Fig. 5*A*), synaptic adhesion molecule FasII (Fig. 5*B*), synaptic vesicle protein synaptotagmin (Syt) (Fig. 5*C*), and subsynaptic reticulum protein Discs large 1 (DLG, homologous to mammal PSD95) (Fig. 5*D*), and we found that the distribution and level of these proteins appeared normal in *dnlg3* mutants. Previous studies have indicated that Nlgs are important for synaptic targeting of postsynaptic receptors (32, 33). We also examined postsynaptic receptors; at NMJs, there are two subtypes of glutamate receptors characterized by the presence of either the GluRIIA or GluRIIB subunit together with shared GluRIII, GluRIID, and GluRIIE. GluRIIA- and GluRIIB-containing receptors are spatially segregated but can coexist within individual synapses (34–39). We examined GluRIIA and GluRIIB, respectively. As shown in Fig. 5, *E* and *F*, the level of synaptic GluRIIA, but not GluRIIB, was significantly reduced in *dnlg3* null mutants, compared with controls. Importantly, the reduction in GluRIIA in *dnlg3* null mutants was fully rescued by postsynaptic expression of DNlg3 (Fig. 5*G*). Consistent with this, the reduced GluRIIA subunit was observed in *dnlg3* mutants by Western blotting (Fig. 5*H*). These results suggest that DNlg3 specifically regulates GluRIIA-containing glutamate receptors at NMJs.

Ultrastructural Synaptic Defects in dnlg3 Null Mutants—A reduction in bouton size suggested that the ultrastructure of NMJs might be altered in *dnlg3* mutants. Therefore, we analyzed the structural properties of both presynaptic and postsynaptic components on EM graphs. The overall gross anatomy of the bouton characterized by the presence of T-bars, synaptic vesicles, and PSD could be formed in *dnlg3* null mutants (Fig. 6, *A* and *B*), indicating that DNlg3 was not absolutely required for synaptic formation. Different from the *dnlg1* and *dnlg2* mutants, the relative SSR area was normal in *dnlg3* mutants compared with the WT controls (data not shown), noting that SSR area was significantly reduced in both *dnlg1* and *dnlg2* mutants (19, 20). However, the presynaptic vesicle size and density were changed in *dnlg3* mutants, including reduced vesicle number and increased vesicle size in *dnlg3* mutants (Fig. 6, *B, E, G,* and *J*). Histogram plots of the synaptic vesicle size distribution showed an overall shift in the distribution of synaptic vesicle diameter toward larger values in *dnlg3* mutants (Fig. 6*H*). In addition, the number of large vesicles (>80 nm in diameter, presumably endosomes, called cisternae) (40) were dramatically increased in *dnlg3* mutants (Fig. 6*I*). Importantly,

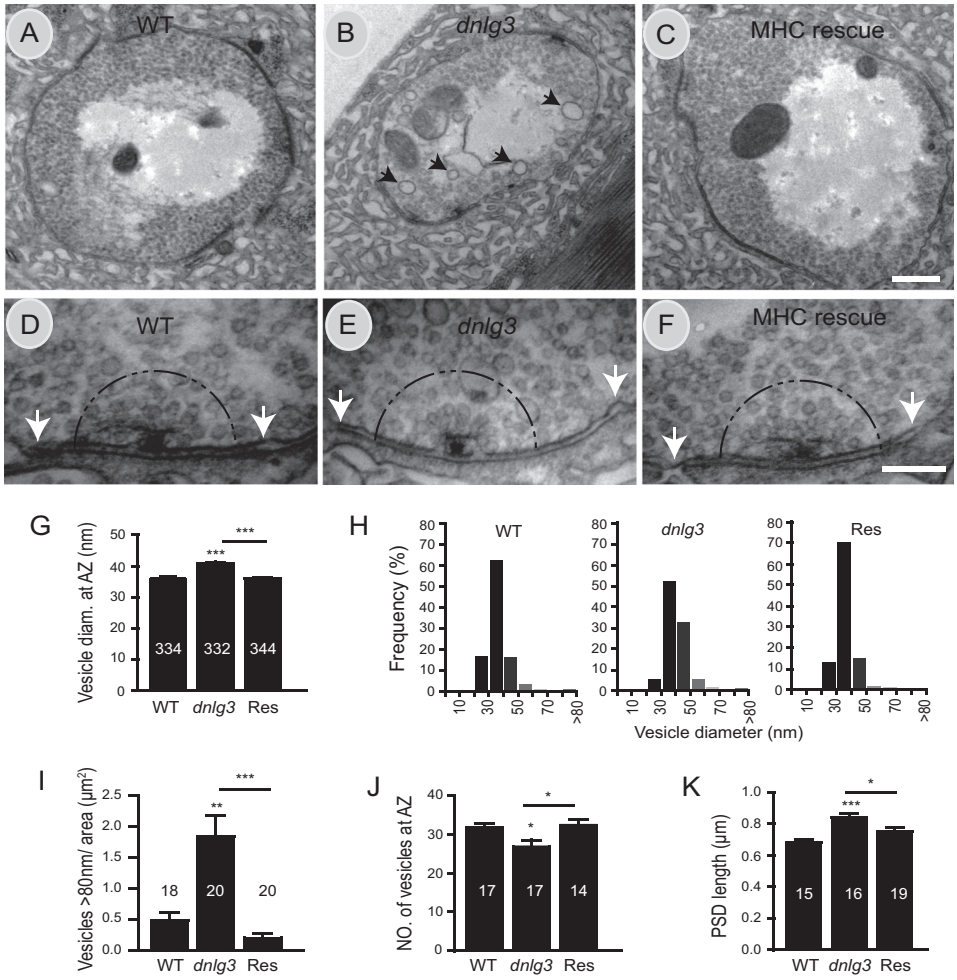

FIGURE 6. **EM analysis of boutons and synaptic structures in *dnlg3* mutants.** *A–F,* EM graphs showing ultrastructures of type Ib boutons at muscle 6/7 in WT, *dnlg3*$^{KO88/f00777}$, and MHC rescue line. *A–C,* low magnification EM images of synaptic boutons. Synaptic vesicles, T-bar, SSR normally formed in WT, *dnlg3* mutant, and Res lines. Note that large vesicles (>80 nm in diameter; called cisternae) are marked by *black arrows* in *B*. *D–F,* high magnification views of active zone, synaptic vesicle, PSD in WT, *dnlg3* mutants, and MHC rescue. Note the 250-nm radius around the T-bar and PSD boundary were marked by a *semicircle* and *white arrows*. *G,* summary *graphs* showing mean vesicle diameter in WT, *dnlg3* mutants, and MHC rescue (*Res*) line. Note that vesicles <80 nm in diameter were included in statistical analysis. *H,* frequency distributions of synaptic vesicle diameter in the defined area around the active zone in WT, *dnlg3* mutants, and MHC rescue (*Res*) lines. *I–K,* summary *graphs* showing the number of large vesicles (cisternae) per μm^2 (*I*); the number of vesicles in a 250-nm radius around the T-bar (*J*); and PSD length (*K*) in WT, *dnlg3* mutant, and rescue line. Note that the number of cisternae was significantly increased in *dnlg3* mutants and could be fully rescued with MHC-Gal4 (*I*); the number of vesicles around the T-bar was significantly reduced in *dnlg3* mutants and could be fully rescued by muscle-specific Gal4 MHC-Gal4 (*J*); the length of PSDs below the presynaptic T-bars was significantly increased in the *dnlg3* mutant, and again this change was partially rescued by the MHC-Gal4 line (*K*). The number of samples analyzed is indicated. *, $p < 0.05$; **, $p < 0.01$; ***, $p < 0.001$, Mann-Whitney test. *Scales bars: A–C,* 0.5 μm; *D–F,* 0.2 μm.

these changes could be fully rescued by muscle expression of DNlg3 (Fig. 6, *G–J*). Interestingly, despite a reduction in bouton size, the length of PSDs was significantly increased in *dnlg3* null mutant compared with the WT control (Fig. 6*K*), and this change was partially rescued by expression of WT DNlg3 with MHC-Gal4 (Fig. 6*K*). Thus, DNlg3 is essential for a proper structural organization of the pre- and postsynaptic site at of NMJs.

Impaired Synaptic Endocytosis in dnlg3 Mutants—Enlarged synaptic vesicles and more cisternaes have been reported in mutants with impaired endocytosis, such as *AP180/lap*, *cyfip*, synaptotagmin, synaptogyrin, *dap160*, *tweek*, and *eps15* mutants (41–47), suggesting that DNlg3 may regulate endocytosis and/or vesicle recycling. To explore whether endocytosis and/or vesicle recycling is altered in *dnlg3* mutants, we turned to the styryl dye FM1-43, which can be taken up in a synaptic vesicle by endocytosis and released by exocytosis. Compared with the wild type, which showed strong dye signaling at the synaptic bouton, *dnlg3* mutants showed a markedly reduced amount of loaded dye (Fig. 7, *A–C*). The relative fluorescent intensity of *dnlg3* mutants was about 70% that of the wild-type controls. We also examined the capacity of *dnlg3* mutants and wild-type boutons to unload dye after 1 min of incubation in high K^+ solution to determine whether exocytosis is impaired in *dnlg3* mutants. Correspondingly, the amount of the remaining dye in *dnlg3* mutants was also reduced compared with wild-type controls (Fig. 7, *B* and *C*). However, the ratio of unloaded to loaded FM1-43 intensity was not different between *dnlg3* mutants and wild-type controls (Fig. 7*D*), indicating that vesicle exocytosis was normal in *dnlg3* mutants. This result suggested that synaptic endocytosis but not exocytosis was impaired in *dnlg3* mutants.

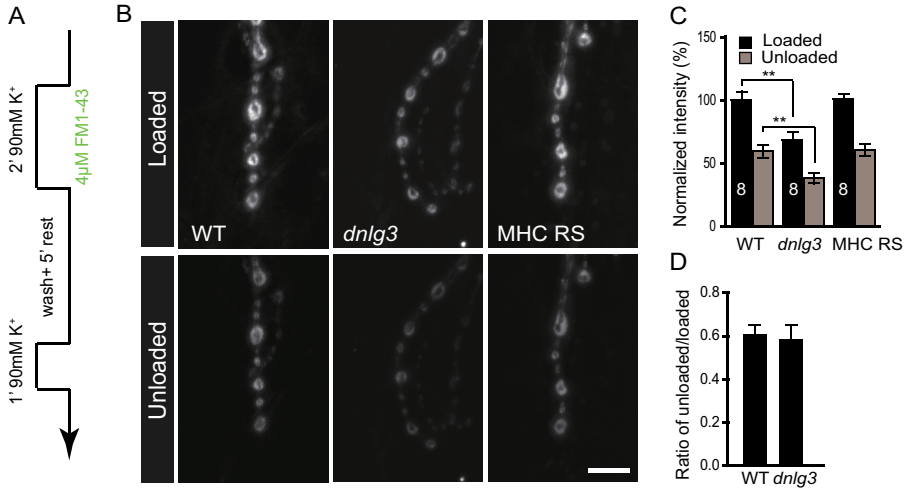

FIGURE 7. **Impaired synaptic endocytosis in *dnlg3* mutants.** *A,* schematic of the FM1-43 loading and unloading protocol. *B,* representative images of boutons loaded with FM1-43 and subsequently unloaded by 90 mM K^+ solution in WT, *dnlg3*$^{KO88/f00777}$, and MHC RS lines. *C,* summary *graph* showing significantly reduced loaded and unloaded FM1-43 dye in *dnlg3* mutants, and the impaired vesicle turnover was rescued by muscle expression of DNlg3 driven by MHC-Gal4. *D,* ratio of unloaded/loaded FM1-43 intensity showed no alteration in *dnlg3* mutants compared with WT. The number of animals analyzed is indicated. **, $p < 0.01$. *Scale bar: B,* 10 μm.

DISCUSSION

Four neuroligin genes have been identified in *Drosophila*. Previous studies have established the role of *dnlg1*, *dnlg2*, and *dnlg4* (19, 20, 22), but the role of DNlg3 had yet to be investigated. In this study, we have shown that DNlg3 played an important role in NMJ development and synaptic maturation. We found that *dnlg3* mutants showed an increase in bouton number and overexpression of DNlg3 with a muscle-specific Gal4 reduced the bouton number, indicating that DNlg3 negatively regulated NMJ growth. At *Drosophila* NMJs, the type I bouton is a glutamatergic synapse similar to mammalian AMPA/kainate synapses. As described above, the fly NMJ glutamate receptors are heterotetrameric complexes composed of GluRIIC, GluRIID, GluRIIE and either GluRIIA or -IIB. The type IIA- and -IIB- containing receptor complex differs in synaptic responses and electrophysiological properties (48). Our results showed that GluRIIA recruitment but not GluRIIB was impaired in *dnlg3* mutants, suggesting that DNlg3 specifically regulated GluRIIA-containing glutamate receptors at NMJs and maybe through direct regulation of the GluRIIA receptor. Ultrastructural results showed that presynaptic vesicle size was increased, and vesicle number was reduced in *dnlg3* mutants, and postsynaptic density maturation was abnormal in *dnlg3* mutants. Correspondingly to the ultrastructural results, we found that synaptic vesicle endocytosis was impaired in *dnlg3* mutants. Consistent with morphological changes, synaptic transmission was altered in *dnlg3* mutants. Both EJP amplitude and mEJP frequency were significantly reduced in *dnlg3* mutants. It seems that reduced EJP amplitude was caused by impaired vesicle endocytosis and reduced GluRIIA targeting, and reduced mEJP frequency was caused by decreased presynaptic vesicle number. Although altered vesicles size and impaired GluRIIA targeting were observed in *dnlg3* mutants, the mEJP amplitudes were not significantly changed. One possible explanation was that unaltered mEJP amplitude was caused by the integral effect of enlarged vesicles and reduced GluRIIA in *dnlg3* mutants. Consistently, previous studies have shown that enlarged vesicles give rise to an increase in mEJP amplitudes (41, 43), and reduced postsynaptic GluRIIA levels result in decreased mEJP amplitudes (35, 36, 49).

It was shown that there are two different sizes of DNlg3 proteins in WT flies by Western blotting assay with antibody against the C-terminal region of DNlg3. One band is around 130 kDa, suggesting that it is likely a full-length DNlg3. The other band is about 90 kDa, which is much smaller than the predicted DNlg3 protein. This phenomenon was also observed in 70-kDa endogenous DNlg2 proteins, which is not coded by alternatively spliced mRNA (20). This indicates that *Drosophila* neuroligins might undergo post-translational processing. In favor of post-translational cleavage of DNlg3, a full-length DNlg3 coding sequence (cDNA of DNlg3) was expressed under neuron-specific Gal4, Elav-Gal4 in WT background. The result showed that protein levels of both two forms were significantly increased in Elav-Gal4 overexpression lines by Western blotting (data not shown), indicating the two forms derived from the full-length DNlg3 protein. More recent studies on mammalian neuroligin1 have shown that neuroligin1 undergoes proteolytic cleavage, and it seems that neuroligin1 cleavage plays important roles in synaptic transmission and spinogenic function (50, 51). It suggests that post-translational processing is a common event in maturation and function in Nlg molecules of vertebrates or invertebrates.

We also note that loss of the *dnlg3* gene gives rise to significantly different effects at NMJs from *dnlg1* or *dnlg2*. These differences are evident in bouton number, bouton morphology, synaptic organization, and receptor composition.

Although similarly to DNlg1 and DNlg2, DNlg3 is also located at glutamatergic boutons, and its effects on bouton development are distinct from DNlg1 and DNlg2. Both *dnlg1* and *dnlg2* null mutants show reduced bouton numbers, and *dnlg1* mutants show increased bouton size (19–21), whereas *dnlg3* null mutants show increased bouton numbers and decreased bouton size (Fig. 4). The *dnlg3* null mutants also exhibit synaptic changes that are distinct from *dnlg1* and *dnlg2*

null mutants. These include impaired presynaptic vesicle endocytosis, increased PSD length (both phenotypes were not observed in *dnlg1* and *dnlg2* mutants), and reduced recruitment of GluRIIA (but not GluRIIB, which is selectively reduced in *dnlg2* null mutants, and some boutons or synapses in *dnlg1* mutants totally lost postsynaptic glutamate receptors, indicating that DNlg1 is involved in both GluRIIA and GluRIIB recruitment). Our results combined with the results of *dnlg1* and *dnlg2* suggest that different members of the DNlg family play different roles in NMJs, and they may regulate NMJs through distinct mechanisms.

Acknowledgments—We thank Dr. Zhengping Jia, Dr. Gabrielle L. Boulianne, and Dr. Moyi Li for useful discussions and critical comments on the manuscript; Dr. A. DiAntonio for anti-DGluR antibodies; the Bloomington Stock Center for providing Drosophila stocks; DSHB for antibodies; and the members of the Xie laboratory for their critical comments on the manuscript.

REFERENCES

1. Chih, B., Engelman, H., and Scheiffele, P. (2005) Control of excitatory and inhibitory synapse formation by neuroligins. *Science* **307,** 1324–1328
2. Scheiffele, P., Fan, J., Choih, J., Fetter, R., and Serafini, T. (2000) Neuroligin expressed in nonneuronal cells triggers presynaptic development in contacting axons. *Cell* **101,** 657–669
3. Nam, C. I., and Chen, L. (2005) Postsynaptic assembly induced by neurexin-neuroligin interaction and neurotransmitter. *Proc. Natl. Acad. Sci. U.S.A.* **102,** 6137–6142
4. Sand, P., Langguth, B., Hajak, G., Perna, M., Prikryl, R., Kucerova, H., Ceskova, E., Kick, C., Stoertebecker, P., and Eichhammer, P. (2006) Screening for neuroligin 4 (NLGN4) truncating and transmembrane domain mutations in schizophrenia. *Schizophr. Res.* **82,** 277–278
5. Sun, C., Cheng, M. C., Qin, R., Liao, D. L., Chen, T. T., Koong, F. J., Chen, G., and Chen, C. H. (2011) Identification and functional characterization of rare mutations of the neuroligin-2 gene (NLGN2) associated with schizophrenia. *Hum. Mol. Genet.* **20,** 3042–3051
6. Jamain, S., Quach, H., Betancur, C., Råstam, M., Colineaux, C., Gillberg, I. C., Soderstrom, H., Giros, B., Leboyer, M., Gillberg, C., Bourgeron, T., and Paris Autism Research International Sibpair Study. (2003) Mutations of the X-linked genes encoding neuroligins NLGN3 and NLGN4 are associated with autism. *Nat. Genet.* **34,** 27–29
7. Araç, D., Boucard, A. A., Ozkan, E., Strop, P., Newell, E., Südhof, T. C., and Brunger, A. T. (2007) Structures of neuroligin-1 and the neuroligin-1/neurexin-1β complex reveal specific protein-protein and protein-Ca^{2+} interactions. *Neuron* **56,** 992–1003
8. Fabrichny, I. P., Leone, P., Sulzenbacher, G., Comoletti, D., Miller, M. T., Taylor, P., Bourne, Y., and Marchot, P. (2007) Structural analysis of the synaptic protein neuroligin and its β-neurexin complex: determinants for folding and cell adhesion. *Neuron* **56,** 979–991
9. Ichtchenko, K., Hata, Y., Nguyen, T., Ullrich, B., Missler, M., Moomaw, C., and Südhof, T. C. (1995) Neuroligin 1: a splice site-specific ligand for β-neurexins. *Cell* **81,** 435–443
10. Graf, E. R., Zhang, X., Jin, S. X., Linhoff, M. W., and Craig, A. M. (2004) Neurexins induce differentiation of GABA and glutamate postsynaptic specializations via neuroligins. *Cell* **119,** 1013–1026
11. Varoqueaux, F., Jamain, S., and Brose, N. (2004) Neuroligin 2 is exclusively localized to inhibitory synapses. *Eur. J. Cell Biol.* **83,** 449–456
12. Budreck, E. C., and Scheiffele, P. (2007) Neuroligin-3 is a neuronal adhesion protein at GABAergic and glutamatergic synapses. *Eur. J. Neurosci.* **26,** 1738–1748
13. Chubykin, A. A., Atasoy, D., Etherton, M. R., Brose, N., Kavalali, E. T., Gibson, J. R., and Südhof, T. C. (2007) Activity-dependent validation of excitatory *versus* inhibitory synapses by neuroligin-1 *versus* neuroligin-2. *Neuron* **54,** 919–931
14. Levinson, J. N., Chéry, N., Huang, K., Wong, T. P., Gerrow, K., Kang, R., Prange, O., Wang, Y. T., and El-Husseini, A. (2005) Neuroligins mediate excitatory and inhibitory synapse formation: involvement of PSD-95 and neurexin-1β in neuroligin-induced synaptic specificity. *J. Biol. Chem.* **280,** 17312–17319
15. Sara, Y., Biederer, T., Atasoy, D., Chubykin, A., Mozhayeva, M. G., Südhof, T. C., and Kavalali, E. T. (2005) Selective capability of SynCAM and neuroligin for functional synapse assembly. *J. Neurosci.* **25,** 260–270
16. Varoqueaux, F., Aramuni, G., Rawson, R. L., Mohrmann, R., Missler, M., Gottmann, K., Zhang, W., Südhof, T. C., and Brose, N. (2006) Neuroligins determine synapse maturation and function. *Neuron* **51,** 741–754
17. Südhof, T. C. (2008) Neuroligins and neurexins link synaptic function to cognitive disease. *Nature* **455,** 903–911
18. Kwon, H. B., Kozorovitskiy, Y., Oh, W. J., Peixoto, R. T., Akhtar, N., Saulnier, J. L., Gu, C., and Sabatini, B. L. (2012) Neuroligin-1-dependent competition regulates cortical synaptogenesis and synapse number. *Nat. Neurosci.* **15,** 1667–1674
19. Banovic, D., Khorramshahi, O., Owald, D., Wichmann, C., Riedt, T., Fouquet, W., Tian, R., Sigrist, S. J., and Aberle, H. (2010) *Drosophila* neuroligin 1 promotes growth and postsynaptic differentiation at glutamatergic neuromuscular junctions. *Neuron* **66,** 724–738
20. Sun, M., Xing, G., Yuan, L., Gan, G., Knight, D., With, S. I., He, C., Han, J., Zeng, X., Fang, M., Boulianne, G. L., and Xie, W. (2011) Neuroligin 2 is required for synapse development and function at the *Drosophila* neuromuscular junction. *J. Neurosci.* **31,** 687–699
21. Chen, Y. C., Lin, Y. Q., Banerjee, S., Venken, K., Li, J., Ismat, A., Chen, K., Duraine, L., Bellen, H. J., and Bhat, M. A. (2012) *Drosophila* neuroligin 2 is required presynaptically and postsynaptically for proper synaptic differentiation and synaptic transmission. *J. Neurosci.* **32,** 16018–16030
22. Li, Y., Zhou, Z., Zhang, X., Tong, H., Li, P., Zhang, Z. C., Jia, Z., Xie, W., and Han, J. (2013) *Drosophila* neuroligin 4 regulates sleep through modulating GABA transmission. *J. Neurosci.* **33,** 15545–15554
23. Gong, W. J., and Golic, K. G. (2003) Ends-out, or replacement, gene targeting in *Drosophila*. *Proc. Natl. Acad. Sci. U.S.A.* **100,** 2556–2561
24. Wermter, A. K., Kamp-Becker, I., Strauch, K., Schulte-Körne, G., and Remschmidt, H. (2008) No evidence for involvement of genetic variants in the X-linked neuroligin genes NLGN3 and NLGN4X in probands with autism spectrum disorder on high functioning level. *Am. J. Med. Genet. B Neuropsychiatr. Genet.* **147B,** 535–537
25. Verstreken, P., Ohyama, T., and Bellen, H. J. (2008) FM 1–43 labeling of synaptic vesicle pools at the *Drosophila* neuromuscular junction. *Methods Mol. Biol.* **440,** 349–369
26. Wang, D., Zhang, L., Zhao, G., Wahlström, G., Heino, T. I., Chen, J., and Zhang, Y. Q. (2010) *Drosophila* twinfilin is required for cell migration and synaptic endocytosis. *J. Cell Sci.* **123,** 1546–1556
27. Li, J., Ashley, J., Budnik, V., and Bhat, M. A. (2007) Crucial role of *Drosophila* neurexin in proper active zone apposition to postsynaptic densities, synaptic growth, and synaptic transmission. *Neuron* **55,** 741–755
28. Zeng, X., Sun, M., Liu, L., Chen, F., Wei, L., and Xie, W. (2007) Neurexin-1 is required for synapse formation and larvae associative learning in *Drosophila*. *FEBS Lett.* **581,** 2509–2516
29. Blundell, J., Tabuchi, K., Bolliger, M. F., Blaiss, C. A., Brose, N., Liu, X., Südhof, T. C., and Powell, C. M. (2009) Increased anxiety-like behavior in mice lacking the inhibitory synapse cell adhesion molecule neuroligin 2. *Genes Brain Behav.* **8,** 114–126
30. Chih, B., Afridi, S. K., Clark, L., and Scheiffele, P. (2004) Disorder-associated mutations lead to functional inactivation of neuroligins. *Hum. Mol. Genet.* **13,** 1471–1477
31. Salazar, A. M., Silverman, E. J., Menon, K. P., and Zinn, K. (2010) Regulation of synaptic Pumilio function by an aggregation-prone domain. *J. Neurosci.* **30,** 515–522
32. Jedlicka, P., Hoon, M., Papadopoulos, T., Vlachos, A., Winkels, R., Poulopoulos, A., Betz, H., Deller, T., Brose, N., Varoqueaux, F., and Schwarzacher, S. W. (2011) Increased dentate gyrus excitability in neuroligin-2-deficient mice *in vivo*. *Cereb. Cortex* **21,** 357–367
33. Mondin, M., Labrousse, V., Hosy, E., Heine, M., Tessier, B., Levet, F., Poujol, C., Blanchet, C., Choquet, D., and Thoumine, O. (2011) Neurexin-neuroligin adhesions capture surface-diffusing AMPA receptors through

PSD-95 scaffolds. *J. Neurosci.* **31,** 13500–13515
34. Schuster, C. M., Ultsch, A., Schloss, P., Cox, J. A., Schmitt, B., and Betz, H. (1991) Molecular cloning of an invertebrate glutamate receptor subunit expressed in *Drosophila* muscle. *Science* **254,** 112–114
35. Petersen, S. A., Fetter, R. D., Noordermeer, J. N., Goodman, C. S., and DiAntonio, A. (1997) Genetic analysis of glutamate receptors in *Drosophila* reveals a retrograde signal regulating presynaptic transmitter release. *Neuron* **19,** 1237–1248
36. DiAntonio, A., Petersen, S. A., Heckmann, M., and Goodman, C. S. (1999) Glutamate receptor expression regulates quantal size and quantal content at the *Drosophila* neuromuscular junction. *J. Neurosci.* **19,** 3023–3032
37. Marrus, S. B., and DiAntonio, A. (2004) Preferential localization of glutamate receptors opposite sites of high presynaptic release. *Curr. Biol.* **14,** 924–931
38. Featherstone, D. E., Rushton, E., Rohrbough, J., Liebl, F., Karr, J., Sheng, Q., Rodesch, C. K., and Broadie, K. (2005) An essential *Drosophila* glutamate receptor subunit that functions in both central neuropil and neuromuscular junction. *J. Neurosci.* **25,** 3199–3208
39. Qin, G., Schwarz, T., Kittel, R. J., Schmid, A., Rasse, T. M., Kappei, D., Ponimaskin, E., Heckmann, M., and Sigrist, S. J. (2005) Four different subunits are essential for expressing the synaptic glutamate receptor at neuromuscular junctions of *Drosophila*. *J. Neurosci.* **25,** 3209–3218
40. Matta, S., Van Kolen, K., da Cunha, R., van den Bogaart, G., Mandemakers, W., Miskiewicz, K., De Bock, P. J., Morais, V. A., Vilain, S., Haddad, D., Delbroek, L., Swerts, J., Chávez-Gutiérrez, L., Esposito, G., Daneels, G., Karran, E., Holt, M., Gevaert, K., Moechars, D. W., De Strooper, B., and Verstreken, P. (2012) LRRK2 controls an EndoA phosphorylation cycle in synaptic endocytosis. *Neuron* **75,** 1008–1021
41. Zhang, B., Koh, Y. H., Beckstead, R. B., Budnik, V., Ganetzky, B., and Bellen, H. J. (1998) Synaptic vesicle size and number are regulated by a clathrin adaptor protein required for endocytosis. *Neuron* **21,** 1465–1475
42. Poskanzer, K. E., Fetter, R. D., and Davis, G. W. (2006) Discrete residues in the c(2)b domain of synaptotagmin I independently specify endocytic rate and synaptic vesicle size. *Neuron* **50,** 49–62
43. Zhao, L., Wang, D., Wang, Q., Rodal, A. A., and Zhang, Y. Q. (2013) *Drosophila* cyfip regulates synaptic development and endocytosis by suppressing filamentous actin assembly. *PLoS Genet.* **9,** e1003450
44. Stevens, R. J., Akbergenova, Y., Jorquera, R. A., and Littleton, J. T. (2012) Abnormal synaptic vesicle biogenesis in *Drosophila* synaptogyrin mutants. *J Neurosci* **32,** 18054–18067
45. Koh, T. W., Korolchuk, V. I., Wairkar, Y. P., Jiao, W., Evergren, E., Pan, H., Zhou, Y., Venken, K. J., Shupliakov, O., Robinson, I. M., O'Kane, C. J., and Bellen, H. J. (2007) Eps15 and Dap160 control synaptic vesicle membrane retrieval and synapse development. *J. Cell Biol.* **178,** 309–322
46. Verstreken, P., Ohyama, T., Haueter, C., Habets, R. L., Lin, Y. Q., Swan, L. E., Ly, C. V., Venken, K. J., De Camilli, P., and Bellen, H. J. (2009) Tweek, an evolutionarily conserved protein, is required for synaptic vesicle recycling. *Neuron* **63,** 203–215
47. Koh, T. W., Verstreken, P., and Bellen, H. J. (2004) Dap160/intersectin acts as a stabilizing scaffold required for synaptic development and vesicle endocytosis. *Neuron* **43,** 193–205
48. DiAntonio, A. (2006) Glutamate receptors at the *Drosophila* neuromuscular junction. *Int. Rev. Neurobiol.* **75,** 165–179
49. Liebl, F. L., and Featherstone, D. E. (2008) Identification and investigation of *Drosophila* postsynaptic density homologs. *Bioinform. Biol. Insights* **2,** 369–381
50. Suzuki, K., Hayashi, Y., Nakahara, S., Kumazaki, H., Prox, J., Horiuchi, K., Zeng, M., Tanimura, S., Nishiyama, Y., Osawa, S., Sehara-Fujisawa, A., Saftig, P., Yokoshima, S., Fukuyama, T., Matsuki, N., Koyama, R., Tomita, T., and Iwatsubo, T. (2012) Activity-dependent proteolytic cleavage of neuroligin-1. *Neuron* **76,** 410–422
51. Peixoto, R. T., Kunz, P. A., Kwon, H., Mabb, A. M., Sabatini, B. L., Philpot, B. D., and Ehlers, M. D. (2012) Trans-synaptic signaling by activity-dependent cleavage of neuroligin-1. *Neuron* **76,** 396–409